EUROPEAN JOURNAL OF PURE AND APPLIED MATHEMATICS
2025, Vol. 18, Issue 1, Article Number 5640
ISSN 1307-5543 – ejpam.com
Published by New York Business Global

A Numerical Study of Cubic-Quartic Optical Soliton Solutions in Birefringent Fibers

Afrah M. Almalki[1,*], Aisha Alshaery[1], Huda O. Bakodah[1], Alyaa AlQarni[2]

[1] *Department of Mathematics and Statistics, Faculty of Science, University of Jeddah, P.O. Box 80327, Jeddah, Saudi Arabia*
[2] *Department of Mathematics, Faculty of Science, University of Bisha, PO Box 551, Bisha 61922, Saudi Arabia*

Abstract. This study addresses the critical issue of understanding the numerical relevance of cubic-quartic solitonic expressions in birefringent fibers, a topic of increasing significance in the field of nonlinear optics due to its implications for optical communication and signal propagation. The research employs the improved Adomian decomposition scheme, developed to derive a generalized numerical method for solving complex-valued nonlinear evolution equations associated with solitons. The results demonstrate a high level of accuracy and are shown to be in total conformity with the established analytical solutions, found in the existing literature, thereby validating the effectiveness of the proposed numerical approach. Notably, the study reveals that even minor numerical errors can significantly influence the transported signal's power, emphasizing the importance of precision in numerical methods for nonlinear systems.

2020 Mathematics Subject Classifications: 35Q55, 35C07, 78A20, 78M40, 65M99

Key Words and Phrases: Numerical study, decomposition method, improved scheme, optical soliton, cubic-quartic bright solution, birefringent fibers

1. Introduction

The propagation of optical pulses, particularly in optical signal processing, has recently become a highly relevant area of technological interest in the contemporary world. In this context, one can highlight the systematic application of optical fibers across various fields, including modern telecommunications, optical metamaterials, ultrafast signal systems, optoelectronics, and optical switching, to name a few [1, 4, 9, 28, 35]. Certainly, various nonlinear phenomena are associated with these areas of optical relevance, necessitating thorough investigations to uncover significant breakthroughs. Some of these

*Corresponding author.
DOI: https://doi.org/10.29020/nybg.ejpam.v18i1.5640

Email addresses: aalmalki1447.stu@uj.edu.sa (A. M. Almalki), aaal-shaery@uj.edu.sa (A. A. Alshaery), hobakodah@uj.edu.sa (H. O. Bakodah), aqarnry@ub.edu.sa (A. A. AlQarni)

phenomena include optical solitons, supercontinuum generation, phase modulation, stimulated scattering, and parametric scattering processes, among others. Additionally, when considering the field of optical signal processing, it is essential to examine the dynamical characterization of pulse transmission processes, such as wavelength conversion, optical amplification, pulse generation, and multi-wavelength sources, to name a few.

However, in connection with the aforementioned nonlinear wave phenomena, it is important to mention the nonlinear Schrödinger equations (NLSEs) as the governing mathematical model for describing nonlinear wave propagation in optical media [11, 13, 14, 19, 21]. Indeed, recent years have witnessed significant progress in the study of optical waves, primarily in polarization-preserving fibers, with limited contributions to birefringent fibers. In these fibers, the propagation of optical solitons is governed by a coupled system [3, 5, 17, 18, 20, 22, 29–32], which is the focus of the current study. The transmission of optical pulses in birefringent fiber media is characterized by polarization, often caused by variations in fiber diameter, non-uniformities in the fiber, or technical issues such as fiber bends and external stress. These factors lead to various challenges, including polarization mode dispersion, which is primarily characterized by pulse differential group delay [8]. This poses a significant setback for long-distance transmission of pulses through fiber devices, especially over transoceanic and transcontinental distances. Moreover, birefringence in birefringent fibers (BFs) is associated with the splitting of optical pulses into independent orthogonally polarized components, constant group velocities, variable propagation characteristics, and weak circular symmetries. This complexity necessitates that the governing NLSE be expressed as a coupled system of equations [6]. Additionally, the concept of cubic-quartic (CQ) solitons arises from a delicate balance between self-phase modulation and chromatic dispersion (CD), particularly when the CD is relatively low. The restoration of the required equilibrium due to insufficient CD further involves the contributions of the third-order dispersion (3OD) and fourth-order dispersion (4OD) terms. This phenomenon has been referred to as CQ dispersive effects [7, 10], marking a breakthrough discovery in optical fiber communication in 2017, which continues to be relevant today. For further insights, see [27] for a discussion of various analytical solitonic structures featuring CQ nonlinearity.

Nevertheless, the current study intends to utilize the renowned numerical method known as the improved Adomian decomposition method (IADM) to derive a generalized numerical scheme for the approximate solution of the NLSE [33, 34] with CQ nonlinearity in birefringent fibers. IADM [2, 12, 15, 25] is based on the classical Adomian decomposition approach, significantly improved to tackle complex-valued nonlinear evolution equations; see also other related efficient computational procedures in [16, 23, 24, 26]. Additionally, the study seeks to employ certain analytical solitonic expressions related to the governing model to validate the efficacy of the devised numerical scheme. To this end, the recent study by Uddin and Hafez [27] will serve as a benchmark, using their promising new extended direct algebraic method (EDAM) for comparison. Furthermore, the study aims to thoroughly examine the level of error compliance, assessing the conformity of the proposed numerical solutions with the adopted analytical solutions [27]. Various tables and plots will be provided for greater clarity. Besides, among the novelty of the current

study includes enhanced analytical capability, generalization of approach, and the validation of methods among others. In the same vein, one may find various significance of the study to include, among others, alignment with established theories, high accuracy of the proposed numerical scheme, provision of more into nonlinear dynamics and setting solid foundation for future undertaking. What is more, the deployed computational method is only limited to the class of complex-valued evolution equations, being endowed with the imaginary number(s), and applicable to various fields of nonlinear sciences.

Lastly, the manuscript is arranged in the following manner: governing model is described in Section 2; while Section 3 gives the analysis of the model via the IADM. Section 4 gives the Adopted exact solitonic expressions and, Section 5 presents the numerical simulation of the derived CQ NLSE scheme using the adopted improved Adomian decomposition method (IADM). Finally, Section 6 presents some concluding comments and highlights some possible future studies.

2. Governing model

The cubic-quartic nonlinear Schrödinger equation (CQ NLSE), which incorporates the nonlinear Kerr law refractive index governing the propagation of nonlinear waves in optical fiber media, is expressed by the following complex-valued nonlinear evolution equation [33, 34]

$$iu_t + ipu_{xxx} + qu_{xxxx} + r|u|^2u = 0, \tag{1}$$

where $u = u(x,t)$ is the complex–valued wave function that governs the propagation of optical wave in birefringent fibers in the spatial and temporal variables x and t, respectively. In addition, the real constant p is the coefficient of 3OD, while the real constant q denotes the coefficient of 4OD. Furthermore, the constant r in the last term is coefficient of the Kerr law nonlinear refractive index.

Moreover, when Eq. (1) splits into two directions concerning the frame of birefringence to typify the nonlocal conduct in BFs, one thus obtains the following coupled CQ NLSE

$$iu_t + ip_1u_{xxx} + q_1u_{xxxx} + (r_1|u|^2 + s_1|v|^2)u = 0, \tag{2}$$

$$iv_t + ip_2v_{xxx} + q_2v_{xxxx} + (r_2|v|^2 + s_2|u|^2)v = 0, \tag{3}$$

where $u = u(x,t)$, and $v = v(x,t)$ are the respective complex–valued wave functions in the spatial and temporal variables x and t, respectively. The real constants p_1 and p_2 are the respective coefficients of 3OD, while the real constant q_1 and q_2 denote the respective coefficients of 4OD. In addition, r_j and s_j, for $j = 1, 2$ represent the respective coefficients of cross-phase (self-phase) modulation, while discarding the cause of four–wave mixing.

Furthermore, it is customary to convert the outlined coupled CQ NLSE in Eqs. (2)-(3) to more suitable forms, through the utilization of related wave transformation to get hold of the resulting ordinary differential equations (ODEs) [27]. To do so, the following transformation is

$$u(x,t) = y_1(\Xi_j)e^{i\Theta_j(x,t)}, \tag{4}$$

$$v(x,t) = y_2(\Xi_j)e^{i\Theta_j(x,t)}, \tag{5}$$

is sought, where $j = \{\mathcal{B}, \mathcal{L}\}$. Certainly, the functions $y_1(\Xi_j)$, and $y_2(\Xi_j)$ are real-valued, while $\Theta_j(x,t)$ for $j = \{\mathcal{B}, \mathcal{L}\}$ denotes the amplitude and phase parts of the propagating pulse wave, respectively. More explicitly, the new variables $\Xi_{\mathcal{B}}$ and $\Theta_{\mathcal{B}}$ are expressed as follows

$$\Xi_{\mathcal{B}} = \frac{1}{\mu}\left(x + \frac{1}{\Gamma\mu}\right)^{\mu} - \frac{v}{\mu}\left(t + \frac{1}{\Gamma\mu}\right)^{\mu}, \tag{6}$$

$$\Theta_{\mathcal{B}} = -\frac{k}{\mu}\left(x + \frac{1}{\Gamma\mu}\right)^{\mu} + \frac{\omega}{\mu}\left(t + \frac{1}{\Gamma\mu}\right)^{\mu} + \theta_0, \tag{7}$$

while the corresponding $\Xi_{\mathcal{L}}$ and $\Theta_{\mathcal{L}}$ variables are defined as follows

$$\Xi_{\mathcal{L}} = \frac{1}{\mu}x^{\mu} - \frac{v}{\mu}t^{\mu}, \tag{8}$$

$$\Theta_{\mathcal{L}} = -\frac{k}{\mu}x^{\mu} + \frac{\omega}{\mu}t^{\mu} + \theta_0. \tag{9}$$

In addition, the involving wave parameters ν, κ, ω, and θ_0 that appear in the above expressions denote the speed, frequency, wavenumber, and phase constant, sequentially. Moreover, upon judiciously substituting either Eqs. (6)-(7) or Eqs. (8)-(9) into the governing coupled CQ NLSE, earlier expressed in Eqs. (2)-(3), one obtains the resulting ODEs; these ODEs are not reported here for brevity.

3. Description of the IADM

This section employs the IADM to derive the resultant generalized iterative scheme for the coupled CQ NLSE (Eqs. (2)-(3)). The IADM is an enhanced variant of the classical Adomian decomposition method, successfully applied to various mathematical physics models. This method is characterized by high convergence and requires less computational space and time, among other advantages. Furthermore, it is widely used to solve a range of problems in technology and science, including contemporary fields such as fluid and solid mechanics, elastodynamics, optics, material science, and astrophysics, to name a few [2, 12, 15, 25].

In this regard, we begin the implementation of the adopted IADM on Eqs. (2)-(3) by splitting the resulting complex-valued wave functions $u(x,t)$ and $v(x,t)$ as follows

$$u(x,t) = u_1 + iu_2, \quad \text{and} \quad v(x,t) = v_1 + iv_2,$$

where $i = \sqrt{-1}$, and $u_1 = u_1(x,t)$, $u_2 = u_2(x,t)$ and $v_1 = v_1(x,t)$, $v_2 = v_2(x,t)$ are real-valued functions. Therefore, with the above split-functions assumption, one obtains from Eqs. (2)-(3) the following real-valued evolution equations (obtained from the corresponding real and imaginary parts) as in what follows.

For $u(x,t)$ component, one obtains the following equations

$$-u_{2t} - p_1u_{2xxx} + q_1u_{1xxxx} + \left[r_1\left(u_1^2 + u_2^2\right) + s_1\left(v_1^2 + v_2^2\right)\right]u_1 = 0, \tag{10}$$

$$u_{1t} + p_1 u_{1xxx} + q_1 u_{2xxxx} + \left[r_1\left(u_1^2 + u_2^2\right) + s_1\left(v_1^2 + v_2^2\right)\right] u_2 = 0, \tag{11}$$

while the following equations are obtained for $v\left(x,t\right)$ component

$$-v_{2t} - p_2 v_{2xxx} + q_2 v_{1xxxx} + \left[r_2\left(v_1^2 + v_2^2\right) + s_2\left(u_1^2 + u_2^2\right)\right] v_1 = 0, \tag{12}$$

$$v_{1t} + p_2 v_{1xxx} + q_2 v_{2xxxx} + \left[r_2\left(v_1^2 + v_2^2\right) + s_2\left(u_1^2 + u_2^2\right)\right] v_2 = 0. \tag{13}$$

Further, the IADM proceeds to decompose the solution functions $u_1\left(x,t\right)$, $u_2\left(x,t\right)$ and $v_1\left(x,t\right)$, $v_2\left(x,t\right)$ in Eqs. (10)-(13) using the sums of infinite series of the following form

$$u_i(x,t) = \sum_{n=0}^{\infty} u_{i,n}, \quad v_i(x,t) = \sum_{n=0}^{\infty} v_{i,n}, \quad i = 1, 2. \tag{14}$$

where $u_{i,n} = u_{i,n}\left(x,t\right)$, and $v_{i,n} = v_{i,n}\left(x,t\right)$. Furthermore, when expressing Eqs. (10)-(11) and (12)-(13) using an operator notation, which is, replacing $\frac{d}{dt}$ with L_t, one thus obtains the following equations for $u\left(x,t\right)$ component

$$-L_t u_2 - p_1 u_{2xxx} + q_1 u_{1xxxx} + N_2\left(u_1, u_2\right) = 0, \tag{15}$$

$$L_t u_1 + p_1 u_{1xxx} + q_1 u_{2xxxx} + N_1\left(u_1, u_2\right) = 0, \tag{16}$$

and for $v\left(x,t\right)$ component as follows

$$-L_t v_2 - p_2 v_{2xxx} + q_2 v_{1xxxx} + A_2\left(v_1, v_2\right) = 0, \tag{17}$$

$$L_t v_1 + p_2 v_{1xxx} + q_2 v_{2xxxx} + A_1\left(v_1, v_2\right) = 0, \tag{18}$$

where $N_1\left(u_1, u_2\right)$ and $N_2\left(u_1, u_2\right)$ in the $u\left(x,t\right)$ component equations are nonlinear terms, explicitly expressed as follows

$$N_2\left(u_1, u_2\right) = \left[r_1\left(u_1^2 + u_2^2\right) + s_1\left(v_1^2 + v_2^2\right)\right] u_1,$$

$$N_1\left(u_1, u_2\right) = \left[r_1\left(u_1^2 + u_2^2\right) + s_1\left(v_1^2 + v_2^2\right)\right] u_2,$$

while the nonlinear terms $A_1\left(v_1, v_2\right)$ and $A_2\left(v_1, v_2\right)$ in the $v\left(x,t\right)$ component equations are determined as follows

$$A_2\left(v_1, v_2\right) = \left[r_2\left(v_1^2 + v_2^2\right) + s_2\left(u_1^2 + u_2^2\right)\right] v_1,$$

$$A_1\left(v_1, v_2\right) = \left[r_2\left(v_1^2 + v_2^2\right) + s_2\left(u_1^2 + u_2^2\right)\right] v_2.$$

Moreover, upon applying the inversion operator L_t^{-1} of the earlier applied direct linear operator L_t, expressed as $L_t^{-1} = \int_0^t (.)\, dt$ to Eqs. (15)-(18), one obtains from the $u\left(x,t\right)$ component equations as follows

$$u_1\left(x,t\right) = u_1\left(x,0\right) - p_1 L_t^{-1} u_{1xxx} - q_1 L_t^{-1} u_{2xxxx} - L_t^{-1} N_1\left(u_1, u_2\right), \tag{19}$$

$$u_2\left(x,t\right) = u_2\left(x,0\right) - p_1 L_t^{-1} u_{2xxx} + q_1 L_t^{-1} u_{1xxxx} + L_t^{-1} N_2\left(u_1, u_2\right), \tag{20}$$

while the $v(x,t)$ component equations yield the following

$$v_1(x,t) = v_1(x,0) - p_2 L_t^{-1} v_{1xxx} - q_2 L_t^{-1} v_{2xxxx} - L_t^{-1} A_1(v_1, v_2), \tag{21}$$

$$v_2(x,t) = v_2(x,0) - p_2 L_t^{-1} v_{2xxx} + q_2 L_t^{-1} v_{1xxxx} + L_t^{-1} A_2(v_1, v_2). \tag{22}$$

Notably, the initial conditions, $u_1(x,0)$, $u_2(x,0)$ and $v_1(x,0)$, $v_2(x,0)$ appearing in the above coupled system can easily be determined upon referring to the initial solution assumption as follows

$$\left.\begin{aligned} u_1(x,0) = \mathrm{Re}(u(x,t)), u_2(x,0) = \mathrm{Im}(u(x,t)), \\ v_1(x,0) = \mathrm{Re}(v(x,t)), v_2(x,0) = \mathrm{Im}(v(x,t)). \end{aligned}\right\}$$

Nonetheless, and without much delay, the deployed IADM reveals the following generalized recurrent solution for Eqs. (10)-(13), starting with the $u(x,t)$ solution component as follows

$$u_{1,0}(x,t) = u_1(x,0), \tag{23}$$

$$u_{2,0}(x,t) = u_2(x,0), \tag{24}$$

$$u_{1,k+1}(x,t) = -p_1 L_t^{-1}(u_{1,k})_{xxx} - q_1 L_t^{-1}(u_{2,k})_{xxxx} - L_t^{-1}(A_{1,k}), \tag{25}$$

$$u_{2,k+1}(x,t) = -p_1 L_t^{-1}(u_{2,k})_{xxx} + q_1 L_t^{-1}(u_{1,k})_{xxxx} + L_t^{-1}(A_{2,k}), \tag{26}$$

while that of the $v(x,t)$ solution component as follows

$$v_{1,0}(x,t) = v_1(x,0), \tag{27}$$

$$v_{2,0}(x,t) = v_2(x,0), \tag{28}$$

$$v_{1,k+1}(x,t) = -p_2 L_t^{-1}(v_{1,k})_{xxx} - q_2 L_t^{-1}(v_{2,k})_{xxxx} - L_t^{-1}(A_{1,k}), \tag{29}$$

$$v_{2,k+1}(x,t) = -p_2 L_t^{-1}(v_{2,k})_{xxx} + q_2 L_t^{-1}(v_{1,k})_{xxxx} + L_t^{-1}(A_{2,k}), \tag{30}$$

where $A_{1,k}$ and $A_{2,k}$ are the discovered Adomian polynomials, which are to be computationally obtained for $u(x,t)$ component as follows

$$A_{j,n} = \frac{1}{n!}\frac{d^n}{d\lambda^n} N_j\left(\sum_{n=0}^{\infty}\lambda^n u_{1,n}(x,t), \sum_{n=0}^{\infty}\lambda^n u_{2,n}(x,t)\right),$$

while that of $v(x,t)$ component via the following compacted formula

$$A_{j,n} = \frac{1}{n!}\frac{d^n}{d\lambda^n} N_j\left(\sum_{n=0}^{\infty}\lambda^n v_{1,n}(x,t), \sum_{n=0}^{\infty}\lambda^n v_{2,n}(x,t)\right).$$

Lastly, the derived generalized recurrent scheme Eqs. (23)-(30) for the governing coupled CQ NLSE Eqs. (2)-(3) in FBs via the use of the IADM will be numerically simulated in the subsequent section, alongside deploying some known exact analytical structures for justification.

4. Adopted exact solitonic expressions

In light of the significant technological relevance of the NLSE [33, 34] with cubic-quartic nonlinearity - not only in polarization-preserving fibers but also in birefringent fibers, which present a more complex scenario - various researchers have proposed different sets of optical solutions using analytical techniques to enhance the efficiency of optical signal processes. Notably, the recent study by Uddin and Hafez [27] utilized the promising extended direct algebraic method (EDAM) to derive various exact optical solitons for the governing model. This method effectively recasts the governing NLSE into a corresponding ordinary differential equation (ODE), leading to a system of algebraic equations. Consequently, some of the exact optical expressions presented by Uddin and Hafez [27] are adopted in the present study as benchmark analytical solutions, as follows:

Bright soliton

Through the application of the beseeched EDAM, Uddin and Hafez [27] were able to construct the bright soliton expressions for the governing CQ NLSE as follows

$$\left.\begin{aligned} u(x,t) &= \frac{3\Phi}{2}\left(\ln A\right)^2\sqrt{-\frac{10kp_1}{Y_2\mathcal{H}_1}}\left\{1-\left[\tanh_A\left(\sqrt{\Phi}\Xi_j\right)+i\sqrt{\mathcal{M}\mathcal{N}}\,\mathrm{sech_A}\left(\sqrt{\Phi}\Xi_j\right)\right]^2\right\}e^{i\Theta_j},\\ v(x,t) &= \frac{3\Pi\Phi}{2}\left(\ln A\right)^2\sqrt{-\frac{10kp_1}{Y_2\mathcal{H}_1}}\left\{1-\left[\tanh_A\left(\sqrt{\Phi}\Xi_j\right)+i\sqrt{\mathcal{M}\mathcal{N}}\,\mathrm{sech_A}\left(\sqrt{\Phi}\Xi_j\right)\right]^2\right\}e^{i\Theta_j}.\end{aligned}\right\} \tag{31}$$

$$\left.\begin{aligned} u(x,t) &= -\frac{3\Phi}{2}\left(\ln A\right)^2\sqrt{-\frac{10kp_1}{Y_2\mathcal{H}_1}}\left\{1-\left[\tanh_A\left(\sqrt{\Phi}\Xi_j\right)-i\sqrt{\mathcal{M}\mathcal{N}}\,\mathrm{sech_A}\left(\sqrt{\Phi}\Xi_j\right)\right]^2\right\}e^{i\Theta_j},\\ v(x,t) &= -\frac{3\Pi\Phi}{2}\left(\ln A\right)^2\sqrt{-\frac{10kp_1}{Y_2\mathcal{H}_1}}\left\{1-\left[\tanh_A\left(\sqrt{\Phi}\Xi_j\right)-i\sqrt{\mathcal{M}\mathcal{N}}\,\mathrm{sech_A}\left(\sqrt{\Phi}\Xi_j\right)\right]^2\right\}e^{i\Theta_j}.\end{aligned}\right\} \tag{32}$$

$$\left.\begin{aligned} u(x,t) &= -\frac{3\Phi}{2}\left(\ln A\right)^2\sqrt{-\frac{10kp_1}{Y_2\mathcal{H}_1}}\left\{1-\left[\coth_A\left(\sqrt{\Phi}\Xi_j\right)-\sqrt{\mathcal{M}\mathcal{N}}\,\mathrm{csch_A}\left(\sqrt{\Phi}\Xi_j\right)\right]^2\right\}e^{i\Theta_j},\\ v(x,t) &= -\frac{3\Pi\Phi}{2}\left(\ln A\right)^2\sqrt{-\frac{10kp_1}{Y_2\mathcal{H}_1}}\left\{1-\left[\coth_A\left(\sqrt{\Phi}\Xi_j\right)-\sqrt{\mathcal{M}\mathcal{N}}\,\mathrm{csch_A}\left(\sqrt{\Phi}\Xi_j\right)\right]^2\right\}e^{i\Theta_j}.\end{aligned}\right\} \tag{33}$$

Moreover, from the latter exact solitonic expressions, $\Phi > 0$ and $\sigma \neq 0$; while the transformation for Ξ_j and Θ_j for $j = \{\mathcal{B}, \mathcal{L}\}$ were previously stated. In addition, for the full implementation of the analytical, and the governing constraint conditions, interested reader(s) is referred to the good work of Uddin and Hafez [27]. In the same vein, one may equally get the explicit expressions for all the constraints conditions, ensuring the existence for valid solitonic expression in the same reference [27].

5. Results of numerical analysis

This section presents the numerical simulation of the derived CQ NLSE scheme using the adopted IADM. Furthermore, the benchmark analytical solutions referenced in Eqs. (31)-(33) will be used to assess the accuracy of the proposed scheme. Certainly, one automatically obtains the corresponding initial conditions from Eqs. (31)-(33) at $t = 0$; together with the related boundary conditions, specifying the range for the spatial variable x for the computational purpose. Additionally, the well-known absolute error difference formula will be employed to estimate the error difference. In addition, some fixed real values for the involving parameters are assumed for simulating the referred bright soliton Eqs. (31)-(32) as follows: $\mu = 1$, $\alpha = 0.1$, $\lambda = 0.5$, $\sigma = 0.2$, $A = e$, $\mathcal{M} = -0.1$, $\mathcal{N} = 0.5$, $\kappa = 0.1$, $\Pi = 2$, $p_1 = 0.2$, $r_1 = -0.2$, $s_1 = 0.3$, and $\theta_0 = 1$; while the following fixed values are considered for simulating the soliton referred bright soliton Eq. (33): $\mu = 1$, $\alpha = 0.1$, $\lambda = 0.9$, $\sigma = 0.5$, $A = e$, $\mathcal{M} = \mathcal{N} = 1$, $\kappa = 0.1$, $\Pi = 2$, $p_1 = 0.2$, $r_1 = -0.2$, $s_1 = 0.3$, $\theta_0 = 1$.
In addition, the following two cases are considered in the numerical simulation:
Case I: when $j = \mathcal{B}$.
Case II: when $j = \mathcal{L}$.
Thus, without delay, the study reports in what follows some error tables (see Tables 1-6) and the two-dimensional graphical depictions (see Figures 1-12) for the simulated numerical results, assessing the exactness of the proposed IADM with the analytical structures reported by Uddin and Hafez [27] earlier expressed in Eqs. (31)-(33). Certainly, the given tables in Tables 1-6 are self-explanatory, ultimately saying the something that the error increases as time increases. Additionally the resulting solution of the governing CQ model $\{u(x,t), v(x,t)\}$ is depicted in Figures 1-12 under the aforesaid Cases I-II over the interval $-20 \leq x \leq 20$, and for $t = 0,\ 0.5,\ 1$. In addition, the results shown by these figures revealed the adopted IADM is a good approximation tool for solving complex-valued evolution equations; in particular, the CQ NLSE in FBs. A high level of exactness has been noted in all the plots, in addition to the revelation of relatively negligible errors in Tables 1-6. Besides, one notices from the reported tables that the error keeps shrinking as the time grows; while the figures portray perfect agreement between various exact solutions and the contending computational IADM scheme; for more rigorous proofs of convergence of the certain Adomian-based approaches, one is asked to read the good works reported in [16, 23, 24, 26] and the references therewith.

Table 1: Absolute errors between the proposed IADM solution and the exact bright solution Eq. (31) under Case I.

t	Error for $u(x,t)$	Error for $v(x,t)$
0.0	$3.3154743250 \times 10^{-11}$	$4.0522024880 \times 10^{-11}$
0.5	$3.6273088130 \times 10^{-07}$	$7.25359840 \times 10^{-07}$
1.0	$7.244079170 \times 10^{-07}$	$1.4488112510 \times 10^{-06}$

Table 2: Absolute errors between the proposed IADM solution and the exact bright solution Eq. (31) under Case II.

t	Error for $u(x,t)$	Error for $v(x,t)$
0.0	$5.484944780 \times 10^{-11}$	$9.0353010030 \times 10^{-11}$
0.5	$2.4533317260 \times 10^{-07}$	$4.9072878790 \times 10^{-07}$
1.0	$4.9129153530 \times 10^{-07}$	$9.8269962640 \times 10^{-07}$

Table 3: Absolute errors between the proposed IADM solution and the exact bright solution Eq. (32) under Case I.

t	Error for $u(x,t)$	Error for $v(x,t)$
0.0	$3.630370780 \times 10^{-11}$	$3.7097958160 \times 10^{-11}$
0.5	$3.7246380130 \times 10^{-07}$	$7.4502952140 \times 10^{-07}$
1.0	$7.4426980490 \times 10^{-07}$	$1.4885442150 \times 10^{-06}$

Table 4: Absolute errors between the proposed IADM solution and the exact bright solution Eq. (32) under Case II.

t	Error for $u(x,t)$	Error for $v(x,t)$
0.0	$8.8257766890 \times 10^{-11}$	$1.1585211690 \times 10^{-10}$
0.5	$2.4486313850 \times 10^{-07}$	$4.8982667650 \times 10^{-07}$
1.0	$4.8922551670 \times 10^{-07}$	$9.7855005360 \times 10^{-07}$

Table 5: Absolute errors between the proposed IADM solution and the exact bright solution Eq. (33) under Case I.

t	Error for $u(x,t)$	Error for $v(x,t)$
0.0	4.240780×10^{-11}	3.959250×10^{-11}
0.5	$1.686434930 \times 10^{-08}$	$3.3728698590 \times 10^{-08}$
1.0	$3.3672392760 \times 10^{-08}$	$6.7344785610 \times 10^{-08}$

Table 6: Absolute errors between the proposed IADM solution and the exact bright solution Eq. (33) under Case II.

t	Error for $u(x,t)$	Error for $v(x,t)$
0.0	$2.2459764440 \times 10^{-11}$	$4.4919532010 \times 10^{-11}$
0.5	$7.7187785040 \times 10^{-09}$	$1.5437556770 \times 10^{-08}$
1.0	$1.5494033650 \times 10^{-08}$	$3.0988067140 \times 10^{-08}$

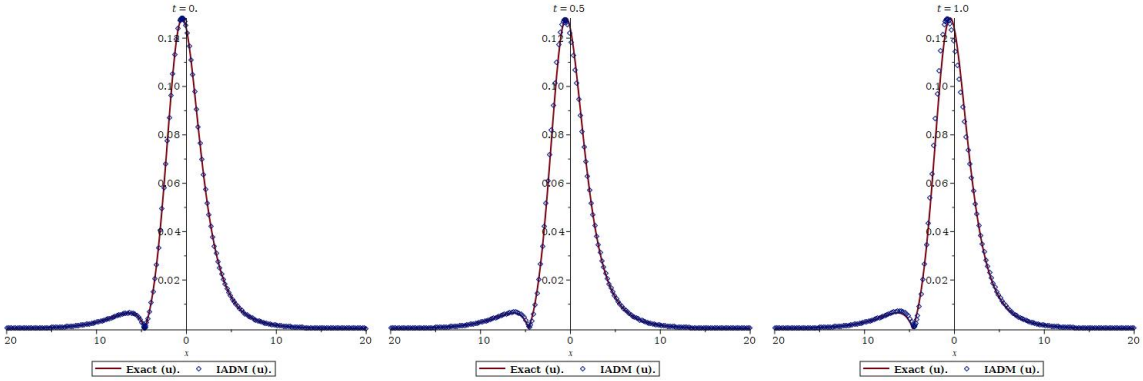

Figure 1: Pictorial depiction, comparing the proposed IADM solution and the exact solution Eq. (31) for the solution pair $u(x,t)$ under Case I.

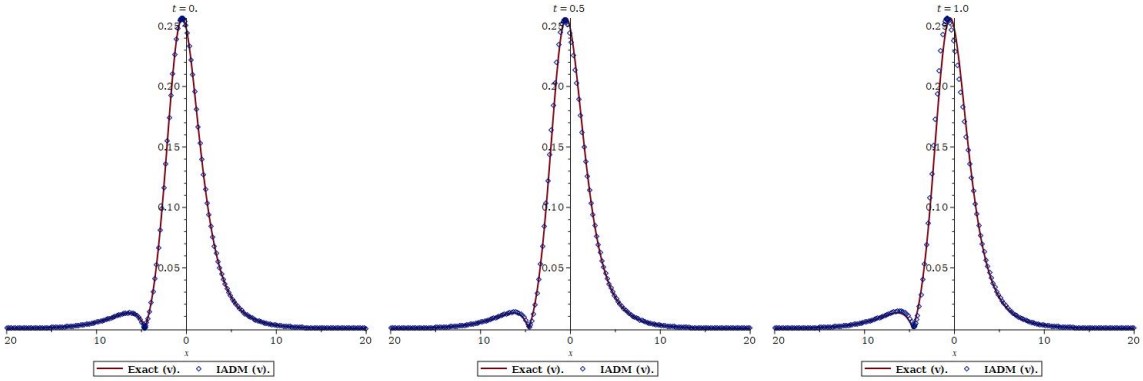

Figure 2: Pictorial depiction, comparing the proposed IADM solution and the exact solution Eq. (31) for the solution pair $v(x,t)$ under Case I.

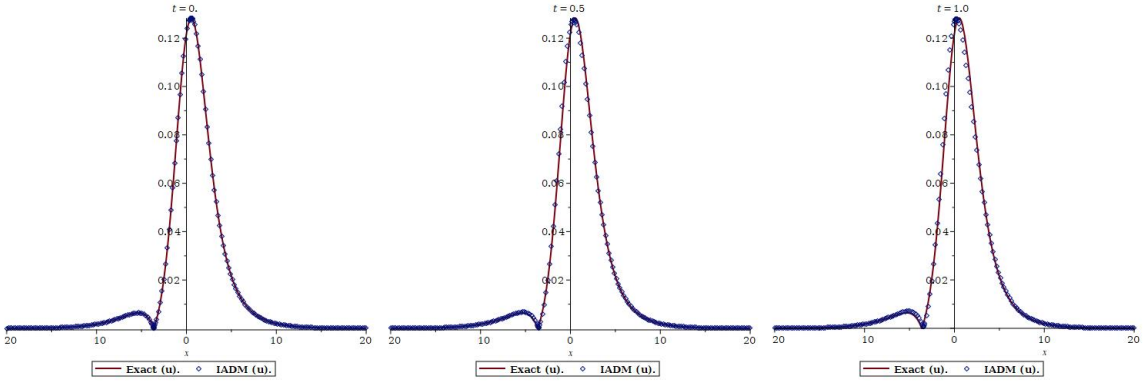

Figure 3: Pictorial depiction, comparing the proposed IADM solution and the exact solution Eq. (31) for the solution pair $u(x,t)$ under Case II.

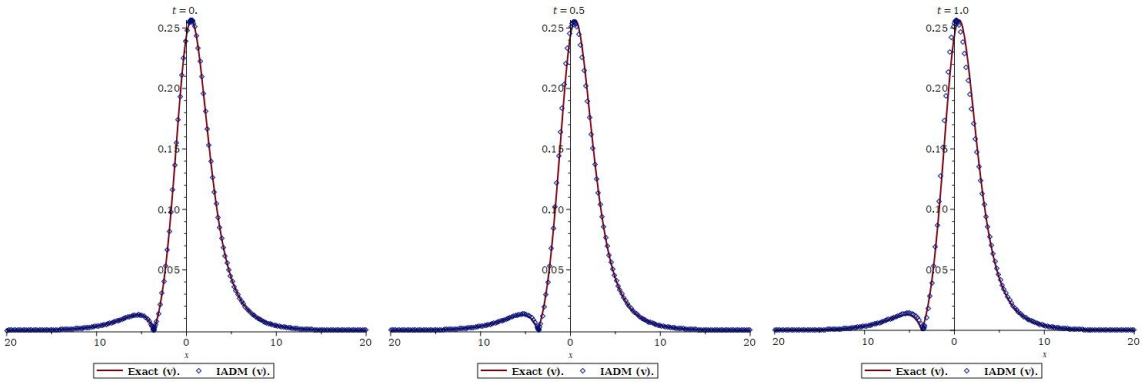

Figure 4: Pictorial depiction, comparing the proposed IADM solution and the exact solution Eq. (31) for the solution pair $v(x,t)$ under Case II.

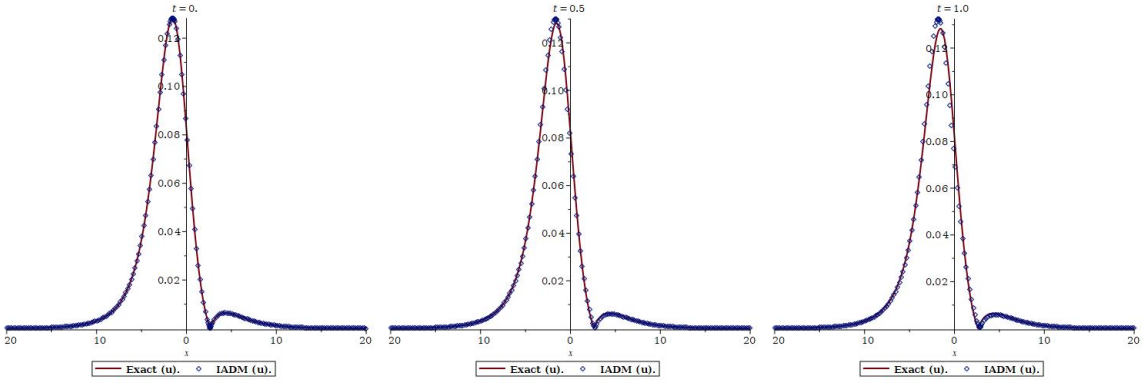

Figure 5: Pictorial depiction, comparing the proposed IADM solution and the exact solution Eq. (32) for the solution pair $u(x,t)$ under Case I.

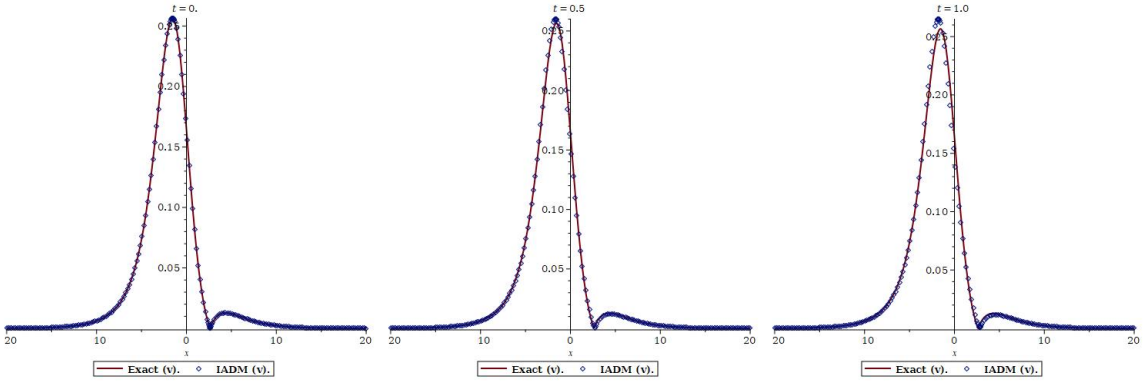

Figure 6: Pictorial depiction, comparing the proposed IADM solution and the exact solution Eq. (32) for the solution pair $v(x,t)$ under Case I.

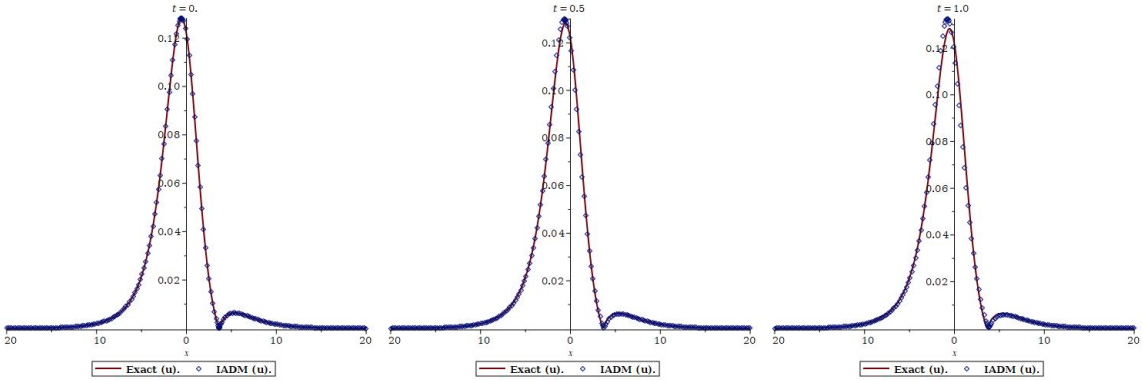

Figure 7: Pictorial depiction, comparing the proposed IADM solution and the exact solution Eq. (32) for the solution pair $u(x,t)$ under Case II.

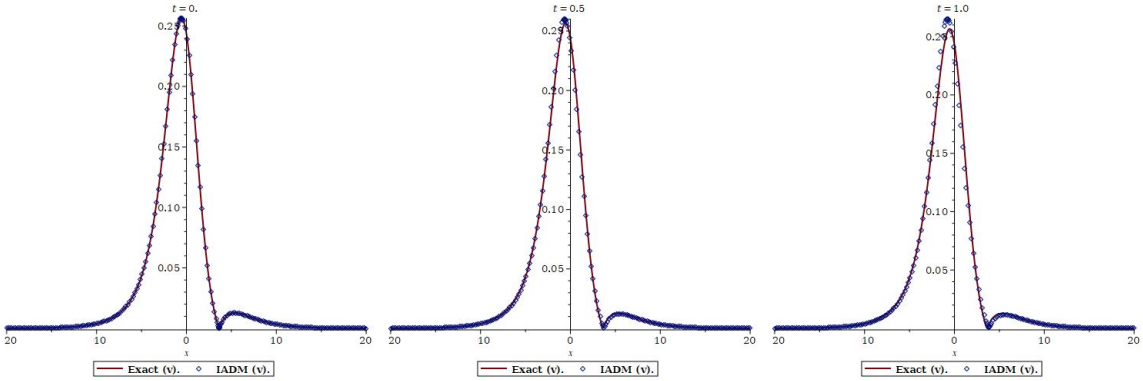

Figure 8: Pictorial depiction, comparing the proposed IADM solution and the exact solution Eq. (32) for the solution pair $v(x,t)$ under Case II.

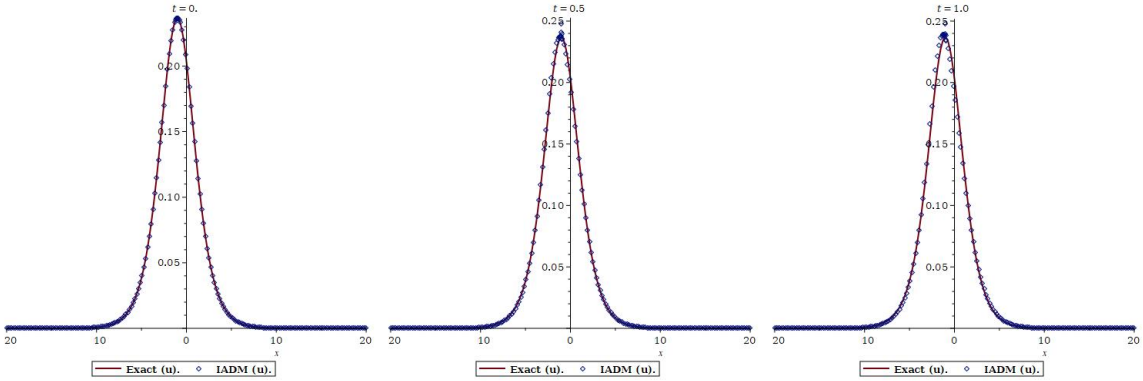

Figure 9: Pictorial depiction, comparing the proposed IADM solution and the exact solution Eq. (33) for the solution pair $u(x,t)$ under Case I.

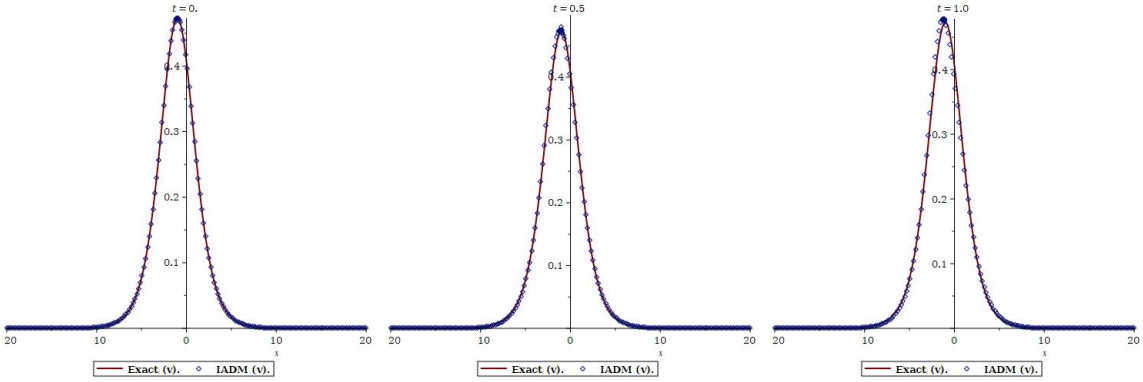

Figure 10: Pictorial depiction, comparing the proposed IADM solution and the exact solution Eq. (33) for the solution pair $v\,(x,t)$ under Case I.

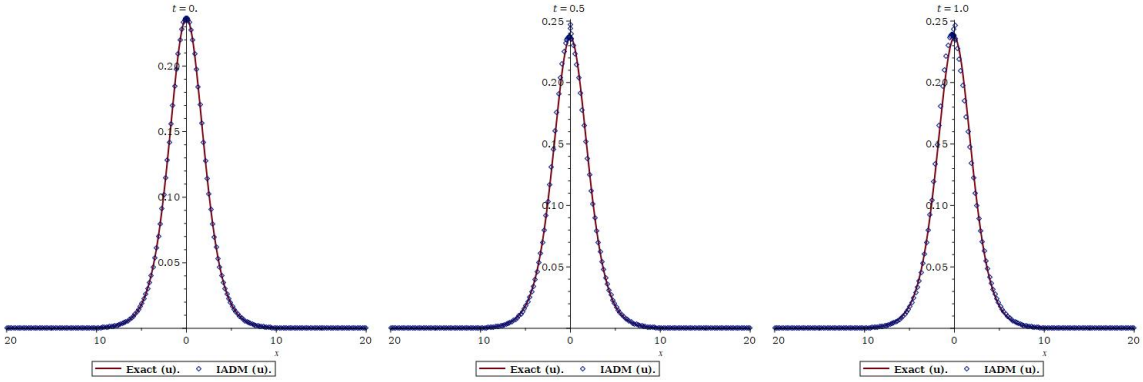

Figure 11: Pictorial depiction, comparing the proposed IADM solution and the exact solution Eq. (33) for the solution pair $u\,(x,t)$ under Case II.

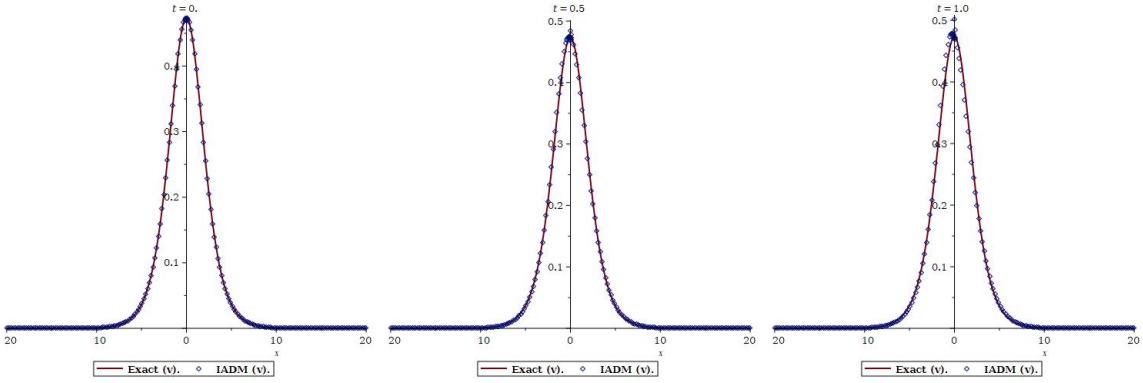

Figure 12: Pictorial depiction, comparing the proposed IADM solution and the exact solution Eq. (33) for the solution pair $v\,(x,t)$ under Case II.

6. Conclusion

Birefringent optical fiber is a significant topic in the realm of optical communication. In this study, we conducted numerical simulations using the promising IADM, which demonstrated high accuracy in results. We focused on the coupled CQ NLSEs exhibiting Kerr-law refractive index nonlinearity to analyze optical pulse transmission in birefringent fibers. Additionally, certain analytically derived soliton solutions proposed by the EDAM were used as benchmark solutions for validation. The proposed IADM scheme effectively approximated the sought-after analytical structures. Moreover, considering the relative error associated with the devised numerical scheme, the study concludes that the application of the proposed method should be extended to high-order complex-valued evolutionary equations involving various nonlinearities. Furthermore, this study aims to provide insights into the dynamics of pulse propagation in birefringent fibers, particularly in relation to changes in fiber diameter, non-uniformities, and other technical defects. Looking ahead, this work paves the way for future research to explore more complex nonlinear interactions and dynamics that arise in different types of fiber materials. It also opens avenues for investigating the influence of external factors, such as varying temperature and fiber configuration, on solitonic behavior. Additionally, the methodology can be adapted to study other nonlinear phenomena in different contexts, potentially leading to innovations in optical technology, and enhanced signal processing applications.

References

[1] G. P. Agrawal. *Nonlinear Fiber Optics*. Academic Press, New York, 2007.

[2] A. Alshaery and A. Ebaid. Accurate analytical periodic solution of the elliptical kepler equation using the adomian decomposition method. *Acta Astronautica*, 140:27–33, 2017.

[3] B. Anjan, Y. Yakup, M. Luminita, I. Catalina, G. P. Lucian, and A. Asim. Optical solitons and complexitons for the concatenation model in birefringent fibers. *Ukrainian Journal of Physical Optics*, 24(4), 2023.

[4] A. H. Arnous, A. Biswas, A. H. Kara, Y. Yıldırım, L. Moraru, C. Iticescu, and A. A. Alghamdi. Optical solitons and conservation laws for the concatenation model with spatio-temporal dispersion (internet traffic regulation). *Journal of the European Optical Society-Rapid Publications*, 19(2):35, 2023.

[5] Y. Barad and Y. Silberberg. Polarization evolution and polarization instability of solitons in a birefringent optical fiber. *Physical Review Letters*, 78(17):3290–3293, 1997.

[6] A. H. Bhrawy, A. A. Alshaery, and E. M. Hilal et al. Optical solitons in birefringent fibers with spatio-temporal dispersion. *Optik*, 125(17):4935–4944, 2014.

[7] A. Biswas, A. H. Kara, M. Z. Ullah, Q. Zhou, H. Triki, and M. Belic. Conservation laws for cubic-quartic optical solitons in kerr and power law media. *Optik*, 145:650–654, 2017.

[8] A. Biswas, K. R. Khan, A. Rahman, A. Yildirim, T. Hayat, and O. M. Aldossary.

Bright and dark optical solitons in birefringent fibers with hamiltonian perturbations and kerr law nonlinearity. *Journal of Optoelectronics and Advanced Materials*, 14:571–576, 2012.

[9] A. Biswas and S. Konar. *Introduction to Non-Kerr Law Optical Solitons*. Chapman and Hall/CRC Press, New York, 2006.

[10] A. Biswas, H. Triki, Q. Zhou, S. P. Moshokoa, M. Z. Ullah, and M. Belic. Cubic-quartic optical solitons in kerr and power law media. *Optik*, 144:357–362, 2017.

[11] A. Biswas, Q. Zhou, M. Z. Ullah, H. Triki, S. P. Moshokoa, and M. Belic. Optical soliton perturbation with anti-cubic nonlinearity by semi-inverse variational principle. *Optik*, 143:131–134, 2017.

[12] A. M. Bodaqah, A. A. Al Qarni, H. O. Bakodah, and A. A. Alshaery. Acquisition of optimal computational solitons for cubic–quartic nonlinear schrödinger equation through improved adomian decomposition method. *Optical and Quantum Electronics*, 56(7):1250, 2024.

[13] R. A. El-Nabulsi and W. Anukool. A generalized nonlinear cubic-quartic schrodinger equation and its implications in quantum wire. *The European Physical Journal B*, 96(5):52, 2023.

[14] M. Eslami. Solitary wave solutions for perturbed nonlinear schrodinger's equation with kerr law nonlinearity under the dam. *Optik*, 126(13):1312–1317, 2015.

[15] O. González-Gaxiola. Numerical solution for triki-biswas equation by adomian decomposition method. *Optik*, 194:163014, 2019.

[16] G. H. Ibraheem, M. Turkyilmazoglu, and M. A. Al-Jawary. Novel approximate solution for fractional differential equations by the optimal variational iteration method. *Journal of Computational Science*, 64:101841, 2022.

[17] M. N. Islam, C. D. Poole, and J. P. Gordon. Soliton trapping in birefringent optical fibers. *Optics Letters*, 14(18):1011–1013, 1989.

[18] Y. Jiang, B. Tian, W. J. Liu, K. Sun, and P. Wang. Mixed-type solitons for the coupled higher-order nonlinear schrödinger equations in multi-mode and birefringent fibers. *Journal of Modern Optics*, 60(8):629–636, 2013.

[19] J. G. Liu, M. S. Osman, and A. M. Wazwaz. A variety of nonautonomous complex wave solutions for the (2+1)-dimensional nonlinear schrodinger equation with variable coefficients in nonlinear optical fibers. *Optik*, 180:917–923, 2019.

[20] C. R. Menyuk. Stability of solitons in birefringent optical fibers. i: equal propagation amplitudes. *Optics Letters*, 12(8):614–616, 1987.

[21] S. Ozgul, M. Turan, and A. Yildirim. Exact traveling wave solutions of perturbed nonlinear schrodinger's equation (nlse) with kerr law nonlinearity. *Optik*, 123(24):2250–2253, 2012.

[22] M. S. Mani Rajan, J. Hakkim, A. Mahalingam, and A. Uthayakumar. Dispersion management and cascade compression of femtosecond nonautonomous soliton in birefringent fiber. *The European Physical Journal D*, 67(7):150, 2013.

[23] M. Turkyilmazoglu. An analytic shooting-like approach for the solution of nonlinear boundary value problems. *Mathematical and Computer Modelling*, 53(9–10):1748–1755, 2011.

[24] M. Turkyilmazoglu. Solution of initial and boundary value problems by an effective accurate method. *International Journal of Computational Methods*, 14(6):1750069, 2017.

[25] M. Turkyilmazoglu. Accelerating the convergence of adomian decomposition method (adm). *Journal of Computational Science*, 31:54–59, 2019.

[26] M. Turkyilmazoglu. Nonlinear problems via a convergence accelerated decomposition method of adomian. *Computer Modeling in Engineering Sciences*, 127(1):1–22, 2021.

[27] M. F. Uddin and M. G. Hafez. Optical wave phenomena in birefringent fibers described by space-time fractional cubic-quartic nonlinear schrödinger equation with the sense of beta and conformable derivative. *Advances in Mathematical Physics*, 2022(1):7265164, 2022.

[28] M. F. Uddin, M. G. Hafez, Z. Hammouch, H. Rezazadeh, and D. Baleanu. Traveling wave with beta derivative spatial-temporal evolution for describing the nonlinear directional couplers with metamaterials via two distinct methods. *Alexandria Engineering Journal*, 60(1):1055–1065, 2021.

[29] Y. Yildirim. Bright, dark and singular optical solitons to kundu–eckhaus equation having four-wave mixing in the context of birefringent fibers by using of modified simple equation methodology. *Optik*, 182:110–118, 2019.

[30] Y. Yildirim. Optical solitons of biswas-arshed equation in birefringent fibers by trial equation technique. *Optik*, 182:810–820, 2019.

[31] Y. Yildirim. Optical solitons to biswas-arshed model in birefringent fibers using modified simple equation architecture. *Optik*, 182:1149–1162, 2019.

[32] Y. Yildirim, A. Biswas, M. Ekici, H. Triki, O. Gonzalez-Gaxiola, A. K. Alzahrani, and M. R. Belic. Optical solitons in birefringent fibers for radhakrishnan–kundu–lakshmanan equation with five prolific integration norms. *Optik*, 208:164550, 2020.

[33] Y. Yildirim, A. Biswas, and A. J. M. Jawad et al. Cubic-quartic optical solitons in birefringent fibers with four forms of nonlinear refractive index by exp-function expansion. *Results in Physics*, 16, 2020.

[34] Y. Yildirim, A. Biswas, P. Guggilla, F. Mallawi, and M. R. Belic. Cubic-quartic optical solitons in birefringent fibers with four forms of nonlinear refractive index. *Optik*, 203, 2020.

[35] Q. Zhou, D. Yao, F. Chen, and W. Li. Optical solitons in gasfilled, hollow-core photonic crystal fibers with inter-modal dispersion and self-steepening. *Journal of Modern Optics*, 60(10):854–859, 2013.